Closed Loop Identification of an Industrial Robot Containing Flexibilities

Måns Östring, Svante Gunnarsson, Mikael Norrlöf

Division of Automatic Control
Department of Electrical Engineering
Linköpings universitet, SE-581 83 Linköping, Sweden
WWW: http://www.control.isy.liu.se
Email: mans@isy.liu.se, svante@isy.liu.se mino@isy.liu.se

31st October 2001

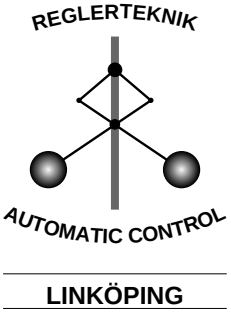

Report No.: LiTH-ISY-R-2398
Submitted to Control Engineering Practice

Abstract

Closed loop identification of an industrial robot of the type ABB IRB 1400 is considered. Using data collected when the robot is subject to feedback control and moving around axis one linear black-box and physically parameterized models are identified. A main purpose is to model the mechanical flexibilities and it is found that the dynamics of the robot can be well approximated by a model consisting of three-masses connected by springs and dampers. It also found that the results of the identification depend on the properties of the input signal.

Keywords: identification, robotics, flexible arms

Closed Loop Identification of an Industrial Robot Containing Flexibilities

Måns Östring, Svante Gunnarsson *, Mikael Norrlöf

Department of Electrical Engineering, Linköping University, SE-58183 Linköping, Sweden

Abstract

Closed loop identification of an industrial robot of the type ABB IRB 1400 is considered. Using data collected when the robot is subject to feedback control and moving around axis one linear black-box and physically parameterized models are identified. A main purpose is to model the mechanical flexibilities and it is found that the dynamics of the robot can be well approximated by a model consisting of three-masses connected by springs and dampers. It also found that the results of the identification depend on the properties of the input signal.

Key words: Identification, Robotics, Flexible arms

1 Introduction

This paper has two purposes. The first one is more application oriented and the aim is to show how identification of physically parameterized models can be used to directly determine the parameters in a linear model describing the dynamic behavior of an industrial robot containing flexibilities. The second purpose is to show an example of identification of a system operating under strong feed-back, i.e. in closed loop. Applying an external excitation signal the input and output signals of the system can be used for direct identification of the input-output dynamics.

System identification is an established tool in engineering in general, see e.g. Ljung (1999) or Söderström and Stoica (1989), and in robotics, see e.g. Kozlowski (1998). Of particular interest here is identification of robots containing

* Corresponding author. Fax:+46-13-282622; Tel: +46-13-281747
Email address: svante@isy.liu.se (Svante Gunnarsson).

flexibilities, and this problem has previously been addressed in for example Dépincé (1998), ElMaraghy et al. (1994), and Nissing and Polzer (2000). The aspects of robot identification that are claimed to be new here are first that the identification is based on closed-loop data collected with the control system operating, and second that the physical parameters are estimated directly instead of determining them indirectly via the parameters of a black-box model. Previous work is presented Östring et al. (2001). The main differences are that the identification is this paper utilize three different data sets which enable cross-validation of the obtained models. A further difference is that the robot is carrying a different load which changes the robot dynamics slightly. Furthermore the excitation signals used here cover a wider frequency range than the one used in Östring et al. (2001). Once and for all it should be observed that the system to be identified is nonlinear. The aim in this paper is however to try to reach as far as possible with linear models of different complexity. Methods for dealing with the nonlinear character of the system are left for future work.

The paper is organized as follows. In Section 2 the robot system under consideration is described briefly, and in Section 3 it is discussed how data have been generated and pre-processed before identification. In Section 4 a linear three-mass model is derived using straightforwards mechanics, and in Section 5 the results from identification using physically parameterized are presented. For comparison the system is also identified using black-box model structures and these results are presented in Section 6. Finally Section 7 contains some conclusions.

2 The Robot System

The robot that is studied in this paper is an industrial robot of the type ABB IRB 1400, and it is shown in Figure 1. In this study only movements around axis one are considered. All other axes are kept at constant positions.

The IRB 1400, which is one of the smaller members in the ABB family, is a six degrees of freedom robot and carries a load of approximately 5 kg. The maximum speed for the TCP (tool center point) is 2.1 m/s and the maximum acceleration is 15 m/s. The robot is equipped with the control system S4C. In addition to the conventional control system an interface between S4C and Matlab has been used. The interface, which is described in Norrlöf (2000), makes it possible to inject and record signals in the robot control system. As described below, it can for example be used to apply suitable excitation signals for identification purposes.

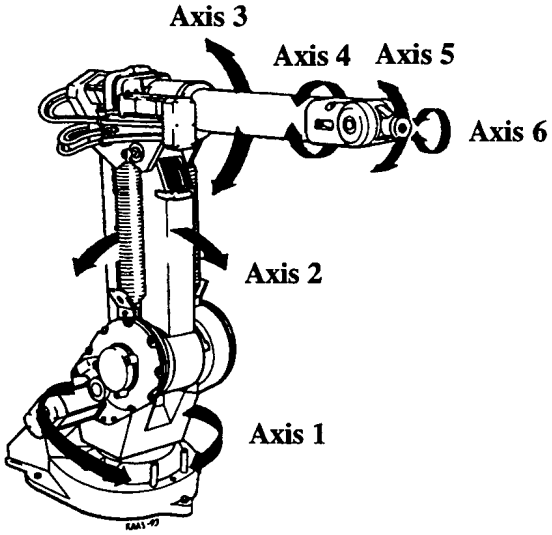

Fig. 1. ABB IRB 1400

3 Data Collection and Pre-processing

3.1 Implementation issues

The data are collected while the control system is in operation. During conventional operation the desired path is specified using a high level programming language. In the control system the desired path and the actual position are used to compute a desired torque which is sent to the motor drive system. The torque then, via gear box and links, results in a movement of the robot arm. Measurements of the actual torque are not available, and instead the torque reference of an inner loop, controlling the motor current, is used. Since the inner control loop has high bandwidth the relationship between torque reference and generated torque can be approximated by a constant. The signals available for measurement for each joint are hence the torque (reference) and the motor angle respectively.The data are collected and sent to a PC using the interface between S4C and Matlab mentioned above.

To obtain suitable excitation of the system an external excitation signal is applied. More specifically the excitation signal is superimposed on the position reference signal which is kept constant during the experiment. An alternative would have been to superimpose the chirp signal on a linearly growing reference signal in order to avoid situations when the velocity changes sign, since the effects of static friction can be a substantial in such cases.

3.2 Experiment design

The determination of excitation signal involves several choices. These are: Number of data N, sampling interval T, and properties of the input signal. An upper bound on the sampling frequency is given by the internal sampling rate in the control system S4C, which is 2 kHz. There is a limitation on the duration of the data collection experiment, but the possible record length of approximately $24 \cdot 10^3$ is judged to be sufficient. The properties of the input signal depend on signal amplitude, frequency content and the shape of the signal. The choice of input signal is crucial in all types of identification for the quality of the identified model. In the area of robot identification this problem has been studied in, for example, Swevers et al. (1997), where however identification of rigid robots is considered. Since the robot considered here contains nonlinearities (back-lash in gear boxes, static friction, etc) the choice of input signal is even more important. The identification experiments reported here are based on three data sets where the excitation signal has different character:

- Set 1: A chirp signal where the frequency changes linearly from 50 to 0.5 Hz in 12 seconds. The resulting input torque has a mean power, measured as $\frac{1}{N}\sum u^2(t)$, of 0.56.
- Set 2: A sum of ten sinusoids with equidistant spacing in frequency, between 5 and 50 Hz. The resulting mean input power is 0.13.
- Set 3: Similar to Set 2, but with larger amplitude. The mean input power is 0.64.

Set 1 and Set 3 have comparable input power but different signal shape, while Set 2 and Set 3 have the same signal shape and different input power. The frequency ranges are approximately the same for all three data sets. It should be noted that even though the excitation signals contain frequencies in the ranges described above the frequency range of the applied torque is also affected by the regulator properties as well the system itself.

3.3 Data pre-processing

It has turned out to be practical to use the motor angle velocity as output instead as the motor angle directly. Therefore the measured motor angle is differentiated numerically before the decimation. In the next step of the preprocessing the sample means are removed, and finally the input and output signals are low-pass filtered, using a fourth order Butterworth filter with cut-off frequency 100 Hz, to emphasize the relevant frequency range.

3.4 Closed Loop Identification

The assumption in this paper is that data are collected while the control system is active, i.e. in closed loop, while the aim is to obtain a model of the open loop system from input torque to motor position. In e.g. Johansson et al. (2000), on the other hand, experiments are presented where the controller is disconnected and the input torques are applied directly.

For identification of systems operating in closed loop there are three main approaches, see Ljung (1999) or Söderström and Stoica (1989): The indirect approach, the joint input-output approach, and the direct approach respectively. In the indirect approach it is required that the controller is known, and since this is not the case here this approach is not applicable. In the joint input-output approach the controller is estimated, and this is also a difficult task since the structure of the controller is not known, and it is likely that the controller contains nonlinear elements. The direct approach can however be applied and this is the method that will be exploited here.

An important question in close loop identification is how the model quality in general, and the bias distribution i particular, is affected by the feedback. A thorough discussion of this topics is found in e.g. Ljung (1999). The main factors that affect the quality of the estimated model is the level of measurement noise, the properties of the feedback and the use of a noise model. In this application the properties of the feedback is fixed as well as the character of the measurement noise. Therefore it will be of interest to investigate what influence the use of noise model will have.

4 Physical Model

The dynamics of the robot system when moving around axis one will be approximated by a model consisting of three masses connected via springs and dampers as shown in Figure 2. The input is the torque τ generated by the electrical motor, while the output is the motor angle θ_m. The angles of the other masses, θ_g and θ_a respectively, are not measurable.

The physical parameters are defined as follows:

J_m, J_a, J_g	moments of inertia	k_g, k_a	spring constants
f_m, f_a, f_g	viscous friction coefficients	d_g, d_a	dampings
r	gear box ratio ($r = 1/118$)		

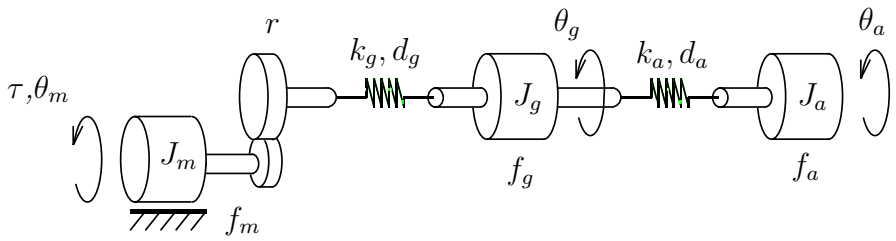

Fig. 2. Three-mass flexible model.

The first mass represents the rotating part of the electrical motor driving the robot, and it is followed by a gear box. The flexibility in the gear box is in the model represented by the spring between the gear box and the second mass. Alternatively the flexibility could be placed before the gear box. The second spring between the second and third mass represents the flexibility in the robot arm.

Applying torque balances for the three masses and introducing the states

$$x(t) = \begin{bmatrix} r\theta_m(t) - \theta_g(t) \\ \theta_g(t) - \theta_a(t) \\ \dot{\theta}_m(t) \\ \dot{\theta}_g(t) \\ \dot{\theta}_a(t) \end{bmatrix} \tag{1}$$

the input signal $u(t) = \tau(t)$ and the output signal $y(t) = \dot{\theta}_m(t)$ give the state space model

$$\dot{x}(t) = Ax(t) + Bu(t) \qquad y = Cx(t) \tag{2}$$

where

$$A = \begin{bmatrix} 0 & 0 & r & -1 & 0 \\ 0 & 0 & 0 & 1 & -1 \\ -\frac{r \cdot k_g}{J_m} & 0 & -\frac{r^2 d_g + f_m}{J_m} & \frac{r \cdot d_g}{J_m} & 0 \\ \frac{k_g}{J_g} & -\frac{k_a}{J_g} & \frac{r d_g}{J_g} & -\frac{f_g + d_g + d_a}{J_g} & \frac{d_a}{J_g} \\ 0 & \frac{k_a}{J_a} & 0 & \frac{d_a}{J_a} & -\frac{d_a + f_a}{J_a} \end{bmatrix} \tag{3}$$

$$B^T = \begin{bmatrix} 0 & 0 & \frac{1}{J_m} & 0 & 0 \end{bmatrix} \qquad C = \begin{bmatrix} 0 & 0 & 1 & 0 & 0 \end{bmatrix} \tag{4}$$

In the robot control system the motor angle θ_m is the only available output signal, but since the measurement noise is fairly small a reasonable estimate of the motor velocity is easily obtained. Therefore the motor velocity is used as output signal in the model above.

To describe the movement of the robot by a fifth order linear model is of course a simplification from different viewpoints. First, the properties of the robot, like e.g. the moments of inertia, depend on the actual position of the robot. In this work the same position is considered in all experiments. Second, it is a simplification to describe the mechanical flexibilities by finite dimensional models, and third, several nonlinearities have been neglected. Some nonlinearities that can be expected to have influence are backlash in the gear-box, nonlinear friction, and nonlinear stiffness in the springs. The approach in this paper is however to stick to linear models and evaluate how well the system can be modeled. The investigation of nonlinear effects, which are left for later publications, include methods to detect nonlinearities using the measured data, insight into how different types of nonlinearities affect the identified models, and finally methods to identify models including nonlinear effects.

5 Identification of Physically Parameterized Models

The identification starts from the state space description on innovations form

$$\dot{x}(t) = A(\theta)x(t) + B(\theta)u(t) + Ke(t) \tag{5}$$
$$y(t) = Cx(t) + e(t) \tag{6}$$

where the matrices $A(\theta), B(\theta)$ and C are given by equation (4) and θ denotes a vector containing the parameters to be identified. Furthermore $e(t)$ is a white noise and K is the Kalman filter gain. Choosing $K = 0$ the model structure corresponds to an output error (OE) structure while $K \neq 0$ denotes that a disturbance model is included. The unknown parameters in the vector θ are estimated using the System Identification Toolbox, see Ljung (2000). Using a priori knowledge the parameters are suitably scaled in order to estimate parameters having the same order of magnitude. Furthermore the inverse of the moments of inertia are introduced as unknown parameters instead of the moments of inertia.

The identification is carried out both $K = 0$ and $K \neq 0$ respectively. This means that in the first case ten physical parameters are identified and in the second case five additional parameters for the noise description are estimated. In Table 1 the value of the loss function of the estimated models are shown for the three data sets and the two model structures. As expected the loss function is much smaller when the noise model is included.

Table 2 shows the results when models are validated using the three data sets. The measure of the fit is given by

$$\text{fit} = 100 \cdot \left(1 - \frac{\sqrt{\sum_{k=1}^{N} (y(t) - \hat{y}(t))^2}}{\sqrt{\sum_{k=1}^{N} (y(t) - \bar{y}))^2}} \right) \tag{7}$$

where $y(t)$ is the measured output, $\hat{y}(t)$ is the simulated output and $\bar{y}$ is the mean value of the measured output. In the table case (i, j) denotes the situation when the model is identified using data set i, and validated using data set j. The situation $i = j$ hence means a case when the model is validated using the data set used for estimation. The fit is rather high in all three cases when the fit is computed using the estimation set, i.e. cases $(1, 1), (2, 2)$ and $(3, 3)$ respectively. The fit is also high when a model estimate using Set1 is validated using Set3 and vice versa. In cross-validations including Set2, e.g. validating the model obtained from Set2 using Set3 (case $(2, 3)$, the fit is essentially lower. This is an interesting observation since the only difference between Set2 and Set3 is the lower amplitude in Set2.

Figures 3 and 4 show the amplitude and phase curves of the estimated models. The models obtained using Set1 and Set 3 agree very well in these figures. There is a small deviation for low frequencies and around the second peak. The model from Set2 agrees in the mid frequency range while the deviation is larger in the low frequency range and around the second peak. This difference might be caused be nonlinear effects. It should also be noticed that the excitation in all data sets is very low below 10 Hz due to the feedback.

For control purposes it is important to determine the frequency of the first notch ω_n with high accuracy. In Table 3 the first notch frequency of the identified models are presented. The relationship between the zeros of a continuous time system and the zeros of the corresponding discrete time system is complicated, and simple relationships can only be obtained as the sampling interval tends to zero. See e.g. Åström and Wittenmark (1984). Comparing the continuous time Bode diagram of the models obtained from the identification of the physically parameterized models to the discrete time Bode diagrams from the black box models there is a difference in the location of the first notch. To make a correct comparison the continuous time models are transformed to their discrete time counterparts before the location of the notch frequency is determined. In Table 3 is is seen that when $K = 0$ the notch frequency ω_n is the same for Set 1 and Set 3, while it is lower for Set 2.A possible explanation to the reduction of ω_n for Set 2 is the presence of backlash in the gear box. In Aberger (2000) it is found using simulations that the presence of backlash reduces the first notch frequency. The reduction depends on the width of the backlash and the magnitude of the input signal. When including a noise model $K \neq 0$ the variation in estimated notch frequency is much larger.

The estimates of the physical parameters using the three data sets are shown in Table 4, where some observations can be made. The first six parameters show a fairly stable behavior when estimated using different data sets. Considering Set1 and Set3 the difference is approximately 10% for J_m and f_m while the difference is lower for the spring constants and moments of inertia. For Set2 the variations are somewhat larger. For a corresponding two-mass flexible model the notch frequency ω_n is approximately given by $\omega_n \approx \sqrt{\frac{k}{J_a}}$ where J_a is the moment of inertia of the second mass. For the three-mass model the zeros of the transfer function from input torque to motor angle velocity are approximately (when $d_a = d_g = f_a = f_g = 0$) given by the roots of the polynomial

$$s^4 + (\frac{k_g}{J_g} + 2\frac{k_a}{J_a})s^2 + \frac{k_a k_g}{J_a J_g} = 0 \tag{8}$$

By comparing the results for Set 1 and Set 3 it is found that even though the estimates of the individual physical parameters differ between the data sets the notch frequency ω_n is the same. The estimate of the notch frequency is hence less sensitive for the character of the excitation signal than the individual physical parameters.

Another measure of the accuracy of the estimated models is obtained by plotting the estimated frequency functions together with estimate confidence regions. Figures 5 and 6 show the amplitude curves of the models (using $K = 0$) obtained using Set1 and Set2 respectively. The curves for Set3 are similar to those of Set1. The figures clearly show that the accuracy is lower when using Set2, and this is natural effect due to the lower signal to noise ratio and nonlinear effects.

The variations in f_m can probably be explained by the fact that the friction in reality also consists of static friction, which is not considered here. The variations in J_m are probably explained by the fact that this estimate is affected by the high frequency components of the signals, and that these differ between the data sets.

For two data sets some of the last four damping and friction parameters are negative. This is obviously unrealistic for a physically parameterized linear model, but a possible explanation here is the presence of nonlinearities. This phenomenon need further investigation. The dampings and friction coefficients in general show large variations between the data sets.

6 Black-box identification

Even though a main point of the paper is the use of physically parameterized models black-box models will also be identified for comparison. The starting point in the black-box identification is the general linear model structure, see e.g. Ljung (1999),

$$y(t) = G(q, \theta)u(t) + H(q, \theta)e(t) \tag{9}$$

where $G(q, \theta)$ and $H(q, \theta)$ are transfer operators, q denotes the shift operator $qy(t) = y(t + 1)$, and θ is the vector of parameters to be determined. $u(t)$ and $y(t)$ denote the input and output signals respectively and $e(t)$ is white noise.

Two different model structures will be studied, and these are the output error (OE) structure, defined by

$$G(q, \theta) = \frac{B(q, \theta)}{F(q, \theta)} \qquad H(q, \theta) = 1 \tag{10}$$

and the Box-Jenkins (BJ) structure, respectively, where

$$G(q, \theta) = \frac{B(q, \theta)}{F(q, \theta)} \qquad H(q, \theta) = \frac{C(q, \theta)}{D(q, \theta)} \tag{11}$$

For the model structure in equation (9) the corresponding one-step-ahead predictor is

$$\hat{y}(t, \theta) = H^{-1}(q, \theta)G(q, \theta)u(t) + (1 - H(q, \theta))y(t) \tag{12}$$

The aim is the to find the parameter vector that minimizes the prediction error

$$\varepsilon(t, \theta) = y(t) - \hat{y}(t, \theta) \tag{13}$$

by minimizing a criterion of the type

$$V_N(\theta) = \frac{1}{N}\sum_{t=1}^{N} \varepsilon^2(t, \theta) \tag{14}$$

For the two model structures mentioned above the predictor is a nonlinear function of the parameter vector, which implies that the parameter estimate has to be computed using an iterative search method.

The identification experiments are carried out using the System Identification Toolbox, Ljung (2000). In order to compare with the results using physically parameterized models above the order of the input-output dynamics is five in

all experiments. For the Box-Jenkins models second order noise dynamics was used. Table 5 shows the simulation fit when calculated similarly to how the fit was calculated for the physically parameterized models. The results for the OE-models are almost identical to the results for the physically parameterized models. The results for the BJ-structure are not directly comparable with the results for physically parameterized models with noise model since the noise descriptions are different.

Table 6 shows the first notch frequency of the identified models, and also here the results for the OE-model are very close to the results for physically parameterized models.

When plotting the Bode diagrams of the OE-models these curves are almost identical to the curves obtained for the physically parameterized models. The similarities are also supported by the values of the fit. The physically parameterized and black-box models, e.g. for Set1, can therfore be considered to be the same.

7 Conclusions

Using data collected in closed loop physically parameterized models of the open loop dynamics of an industrial robot have been obtained. The models clearly reveal that the system contains mechanical flexibilities. Even though data are collected in closed loop models without noise description (OE-models) seem to be appropriate for the task. The results show that the input signal properties have influence on the obtained models.

8 Acknowledgments

This work was supported by CENIIT at Linköping University and by ABB Robotics within ISIS at Linköping University.

References

Aberger, M., Dec 2000. Effects of nonlinearities in black box identification of an industrial robot. Tech. Rep. LiTH-ISY-R-2322, Department of Electrical Engineering, Linköping University, SE-581 83 Linköping, Sweden.

Åström, K. J., Wittenmark, B., 1984. Computer Controlled Systems: Theory and Design. Prentice-Hall, Englewood Cliffs, N.J.

Dépincé, P., May 1998. Parameters identification of flexible robots. IEEE Proceedings on Robotics and Automation , 1116–1121.

ElMaraghy, W. H., ElMaraghy, H. A., Zaki, A., Massoud, A., September 1994. A study on the design and control of robot manipulators with flexibilities. In: Fourth IFAC Symposium on Robot Control.

Johansson, R., Robertsson, A., Nilsson, K., Verhaegen, M., 2000. State-space system identification of robot manipulator dynamics. Mechatronics 10, 403–418.

Kozlowski, K., 1998. Modelling and Identification in Robotics. Springer-Verlag.

Ljung, L., 1999. System Identification: Theory for the User, 2nd Edition. Prentice-Hall, Upper Saddle River, N.J. USA.

Ljung, L., 2000. System Identification Toolbox – User's Guide. The MathWorks Inc, Sherborn, MA, USA.

Nissing, D., Polzer, J., 2000. Parameter identification of a substitution model for a flexible link. System Identification Symposium SYSID 2000.

Norrlöf, M., 2000. Iterative learning control. analysis, design and experiments. Ph.D. thesis, Linköping University, Linköping, Sweden.

Söderström, T., Stoica, P., 1989. System Identification. Prentice-Hall International, Hemel Hemptstead, Hertfordshire.

Östring, M., Gunnarsson, S., Norrlöf, M., April 2001. Closed loop identification of physical parameters of an industrial robot. In: 32nd International Symposium on Robotics. Seoul, Korea.

Swevers, J., Ganseman, C., Tükel, D., Schutter, J. D., Brussel, H. V., 1997. "Optimal Robot Excitation and Identification". IEEE Transactions on Robotics and Automation 13, 730–740.

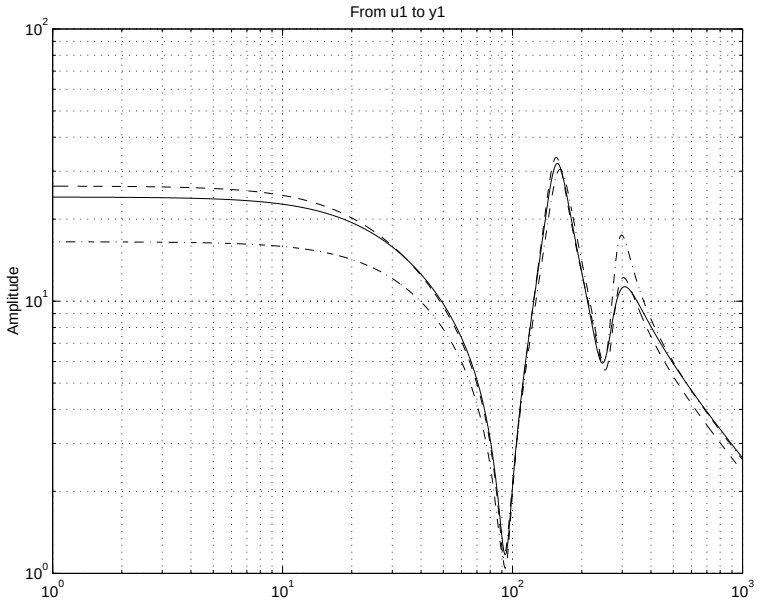

Fig. 3. Amplitude curves of physically parameterized models when $K = 0$. Solid – Set 1, Dashed – Set 3, Dash-dotted – Set 2.

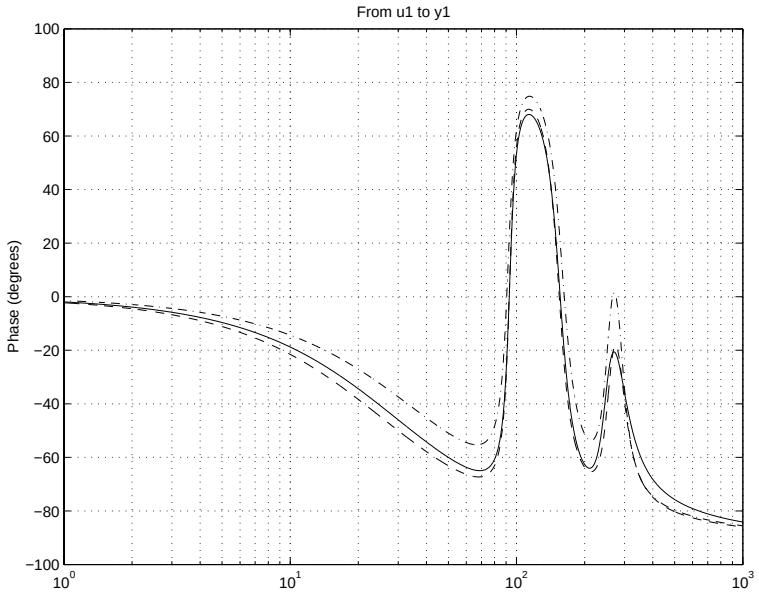

Fig. 4. Phase curves of physically parameterized models when $K = 0$. Solid – Set 1, Dashed – Set 3, Dash-dotted – Set 2.

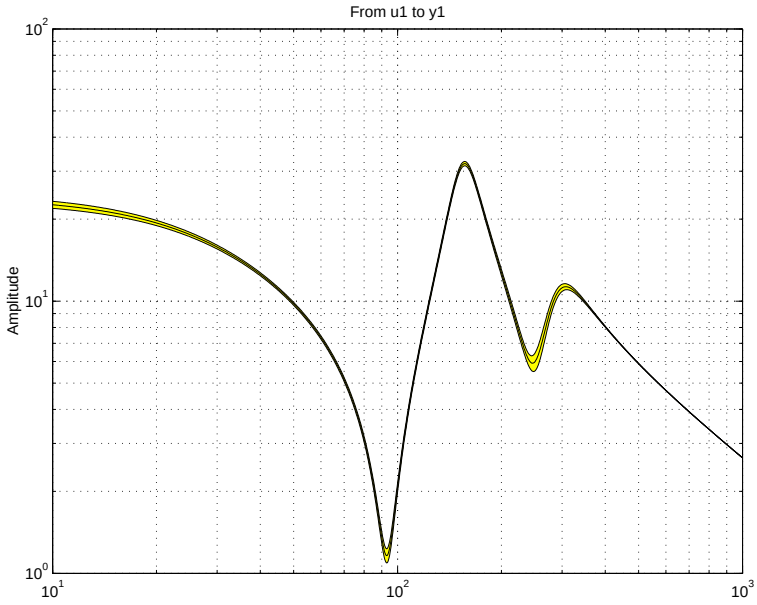

Fig. 5. Amplitude curve and confidence region for the mode obtained using Set1.

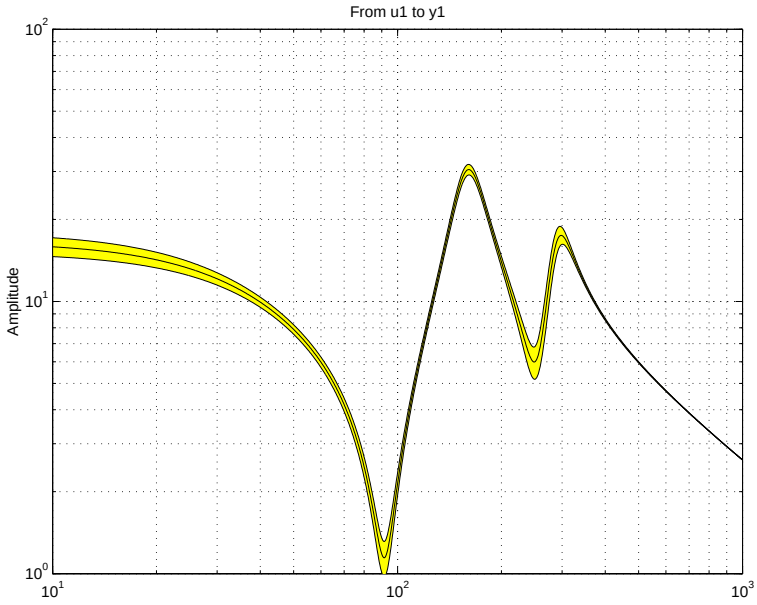

Fig. 6. Amplitude curve and confidence region for the mode obtained using Set2.

Data set	$K = 0$	$K \neq 0$
1	0.83	$9 \cdot 10^{-5}$
2	0.50	$3.7 \cdot 10^{-6}$
3	1.03	$1.2 \cdot 10^{-6}$

Table 1
Loss functions for the physically parameterized models.

Case	$K = 0$	$K \neq 0$
(1,1)	85 %	70 %
(1,2)	66 %	55 %
(1,3)	84 %	70 %
(2,1)	62 %	∞
(2,2)	82 %	∞
(2,3)	62 %	∞
(3,1)	83 %	69 %
(3,2)	65 %	51 %
(3,3)	86 %	70 %

Table 2
Simulated fit according to equation (7) in case (i, j), i.e. when a model estimated using data set i is simulated using data set j.

Data set	$K = 0$	$K \neq 0$
1	93.0	92.2
2	91.5	88.9
3	93.0	91.1

Table 3
Estimate of the first notch frequency ω_n in the Bode diagram for the physically parameterized models.

Par.	Set 1	Set 2	Set 3
J_m	$3.9 \cdot 10^{-4}$	$4.0 \cdot 10^{-4}$	$4.4 \cdot 10^{-4}$
k_g	$1.9 \cdot 10^{5}$	$2.0 \cdot 10^{5}$	$1.9 \cdot 10^{5}$
J_g	6.3	7.2	6.2
f_m	$2.6 \cdot 10^{-2}$	$3.1 \cdot 10^{-2}$	$2.3 \cdot 10^{-2}$
k_a	$1.5 \cdot 10^{5}$	$1.9 \cdot 10^{5}$	$1.6 \cdot 10^{5}$
J_a	12.2	10.3	11.6
d_g	168	-18	91
d_a	-12	-6	21
f_g	232	392	201
f_a	-11	17	8

Table 4
Estimates of physical parameters for different data sets using $K = 0$.

Case	OE	BJ
(1,1)	85 %	82 %
(1,2)	66 %	67 %
(1,3)	83 %	82 %
(2,1)	62 %	45 %
(2,2)	82 %	55 %
(2,3)	62 %	45 %
(3,1)	83 %	53 %
(3,2)	65 %	50 %
(3,3)	86 %	55 %

Table 5
Model fit according to equation (7) in case (i, j), i.e. when a model estimated using data set i is simulated using data set j.

Data set	OE	BJ
1	93.3	94.5
2	91.5	92.8
3	93.0	96.2

Table 6
Estimate of the first notch frequency (rad/s) in the Bode diagram